LETTER

doi:10.1038/nature11836

Ecosystem resilience despite large-scale altered hydroclimatic conditions

Guillermo E. Ponce Campos[1,2], M. Susan Moran[1], Alfredo Huete[3], Yongguang Zhang[1], Cynthia Bresloff[2], Travis E. Huxman[4], Derek Eamus[3], David D. Bosch[5], Anthony R. Buda[6], Stacey A. Gunter[7], Tamara Heartsill Scalley[8], Stanley G. Kitchen[9], Mitchel P. McClaran[10], W. Henry McNab[11], Diane S. Montoya[12], Jack A. Morgan[13], Debra P. C. Peters[14], E. John Sadler[15], Mark S. Seyfried[16] & Patrick J. Starks[17]

Climate change is predicted to increase both drought frequency and duration, and when coupled with substantial warming, will establish a new hydroclimatological model for many regions[1]. Large-scale, warm droughts have recently occurred in North America, Africa, Europe, Amazonia and Australia, resulting in major effects on terrestrial ecosystems, carbon balance and food security[2,3]. Here we compare the functional response of above-ground net primary production to contrasting hydroclimatic periods in the late twentieth century (1975–1998), and drier, warmer conditions in the early twenty-first century (2000–2009) in the Northern and Southern Hemispheres. We find a common ecosystem water-use efficiency (WUE_e: above-ground net primary production/evapotranspiration) across biomes ranging from grassland to forest that indicates an intrinsic system sensitivity to water availability across rainfall regimes, regardless of hydroclimatic conditions. We found higher WUE_e in drier years that increased significantly with drought to a maximum WUE_e across all biomes; and a minimum native state in wetter years that was common across hydroclimatic periods. This indicates biome-scale resilience to the interannual variability associated with the early twenty-first century drought—that is, the capacity to tolerate low, annual precipitation and to respond to subsequent periods of favourable water balance. These findings provide a conceptual model of ecosystem properties at the decadal scale applicable to the widespread altered hydroclimatic conditions that are predicted for later this century. Understanding the hydroclimatic threshold that will break down ecosystem resilience and alter maximum WUE_e may allow us to predict land-surface consequences as large regions become more arid, starting with water-limited, low-productivity grasslands.

Increased aridity and persistent droughts are projected in the twenty-first century for most of Africa, southern Europe and the Middle East, most of the Americas, Australia and South East Asia[1]. This is predicted to change vegetation productivity markedly across ecosystems from grasslands to forests[2,4,5] and affect societal needs for food security and basic livelihood[6]. However, model predictions of productivity responses only provide the most-likely scenarios of the impact of climate change, and few experiments have focused on how anticipated changes in precipitation might be generalized across terrestrial ecosystems. Long-term measurements of natural variability in field settings, supported by manipulative experiments, are considered the best approach for determining the effect of prolonged drought on vegetation productivity[6,7].

In field experiments, vegetation productivity is generally measured as the above-ground net primary production (ANPP, or total new organic matter produced above-ground during a specific interval[8]), and vegetation response to changes in precipitation is quantified as rain-use efficiency (RUE), defined as the ratio of ANPP to precipitation over a defined season or year[9]. Using this approach, continental-scale patterns of RUE have been reported for extended periods in the late twentieth century[10]. Ecosystem water-use efficiency (WUE_e: ANPP/evapotranspiration[11]) provides further insight into the ecological functioning of the land surface, in which evapotranspiration is calculated as precipitation minus the water lost to surface runoff, recharge to groundwater and changes to soil water storage[12] (see Methods). Here we compare the functional responses of RUE and WUE_e to local changes in precipitation to document ecosystem resilience—the capacity to absorb disturbances and retain the same function, feedbacks and sensitivity[13]—during altered hydroclimatic conditions.

The objective was to determine how ANPP across biomes responded to altered hydroclimatic conditions forced by the contemporary drought in Southern and Northern Hemispheres from 2000–2009. Measurements made at 12 US Department of Agriculture (USDA) long-term experimental sites in the conterminous United States and Puerto Rico, and 17 similar sites in the Australian continent over a range of precipitation regimes (termed $USDA_{00-09}$ and $Australia_{01-09}$, respectively). To contrast productivity under altered hydroclimatic conditions with precipitation variability in the late twentieth century, we compared results from the 2000–2009 period with similar analysis of measurements made during the period from 1975–1998 (ref. 10). The latter measurements were primarily from Long-term Ecological Research (LTER) locations, with 14 sites—12 in North America, 2 in Central and South America—hereafter referred to as the $LTER_{75-98}$ data set. For a subset of the $LTER_{75-98}$ sites, ANPP measurements were continued during the period from 2000–2009 (termed $LTER_{00-09}$), and these were used for further validation of the results (see Supplementary Information and Supplementary Table 1).

The warm drought during the early twenty-first century in the United States, Europe and Australia has been recognized as a considerable change from the climatological variability of the late twentieth century[1,14]. Globally, 2000–2009 ranked as the ten warmest years of the 130-year (1880–2009) record[15]. Global annual evapotranspiration increased on average by 7.1 mm yr^{-1} $decade^{-1}$ from 1982–1997, and after that, remained at a plateau through 2008, thus revealing the

[1]USDA ARS Southwest Watershed Research, Tucson, Arizona 85719, USA. [2]Soil, Water & Environmental Sciences, University of Arizona, Tucson, Arizona 85721, USA. [3]Plant Functional Biology and Climate Change Cluster, University of Technology Sydney, New South Wales 2007, Australia. [4]Ecology & Evolutionary Biology, University of California, Irvine, California, USA and Center for Environmental Biology, University of California, Irvine, California 92697, USA. [5]USDA ARS Southeast Watershed Research Laboratory, Tifton, Georgia 31793, USA. [6]USDA ARS Pasture Systems & Watershed Management Research Unit, University Park, Pennsylvania 16802, USA. [7]USDA ARS Southern Plains Range Research Station, Woodward, Oklahoma 73801, USA. [8]USDA FS International Institute of Tropical Forestry, Rio Piedras 00926, Puerto Rico. [9]USDA FS Rocky Mountain Research Station Shrub Sciences Laboratory, Provo, Utah 84606, USA. [10]School of Natural Resources & the Environment, University of Arizona, Tucson, Arizona 85721, USA. [11]USDA FS Southern Research Station, Asheville, North Carolina 28806, USA. [12]USDA FS Pacific Southwest Research Station, Arcata, California 95521, USA. [13]USDA ARS Rangeland Resources Research Unit, Fort Collins, Colorado 80526, USA. [14]USDA ARS Jornada Experimental Range & Jornada Basin Long Term Ecological Research Program, New Mexico State University, Las Cruces, New Mexico 88012, USA. [15]USDA ARS Cropping Systems & Water Quality Research Unit, Columbia, Missouri 65211, USA. [16]USDA ARS Northwest Watershed Research Center, Boise, Idaho 83712, USA. [17]USDA ARS Grazinglands Research Laboratory, El Reno, Oklahoma 73036, USA.

impact of the drought on this important Earth surface process[16]. In the United States, heatwaves in 2005, 2006 and 2007 broke all-time records for high maximum and minimum temperatures, and drier than average conditions were reported for more than 50% of the conterminous United States in 2000–2002 and 2006–2007 (ref. 17). In Australia, the widespread six-year drought from 2001 to 2007 is considered the most severe in the nation's history[18]. The mean Palmer Drought Severity Index (PDSI; see Methods) for USDA and Australian sites decreased significantly ($P < 0.002$) from 1980–1999 to 2000–2009 (USDA) and to 2001–2009 (Australia), declining from −0.06 to −0.81 and from 0.09 to −1.34, respectively, where a reduction in the PDSI indicates an increase in aridity. Furthermore, warm-season temperatures at USDA and Australian sites during the 2000–2009 periods were significantly higher ($P < 0.014$) than 1980–1999 averages, warming by 0.32 and 0.44 °C, respectively.

The enhanced vegetation index (EVI)[19] satellite observations from the Moderate Resolution Imaging Spectroradiometer (MODIS) were integrated annually (termed iEVI) as an empirical proxy for ANPP at $USDA_{00–09}$ and $Australia_{01–09}$ sites (see Methods). Several publications suggest that this is a robust approximation of collective plant behaviour[20], and in this study, we quantified the accuracy of this relationship for the biomes and precipitation patterns. *In situ* estimates of ANPP made with conventional field methods ($ANPP_G$) between 2000 and 2009 were compiled for ten sites across the United States (see Supplementary Information and Supplementary Table 2) and compared with iEVI measurements for the same site and year (Fig. 1). A log–log regression equation was used to estimate ANPP from iEVI values ($ANPP_S$), in which $ANPP_S = 51.42 \times iEVI^{1.15}$ (Fig. 1).

The response of plant production to precipitation during the contemporary hydroclimatic conditions of prolonged warm drought showed strong agreement with the ANPP/precipitation relations reported during the late twentieth century[10] (Fig. 2a). The lowest mean RUE (that is, the slope of the ANPP/precipitation relationship) reported for biomes with the highest mean precipitation can be explained largely (although not completely[10]) by the rain water that is not available for plant production owing to runoff, groundwater recharge and increased soil water storage. Thus, the increase in water available for vegetation production with increasing precipitation is partially consumed by non-biological components of the hydrological cycle (that is, runoff and deep drainage). This becomes apparent when production was plotted as a function of evapotranspiration: the mean ecosystem water-use efficiency (WUE_m) was constant across the entire precipitation gradient (Fig. 2b). Furthermore, there were no significant differences among WUE_m for the three data sets ($P > 0.05$ per homogeneity of regression slope test). Combined, this indicated that all biomes retained their intrinsic sensitivity to water availability during prolonged, warm drought conditions. This suggests that the rules governing how species are organized in terms of their tolerance of hydrological stress are robust despite extended perturbation by low precipitation.

When water limitations at each site were most severe (for the driest years in each multi-year record), a maximum ecosystem WUE (WUE_x) across all biomes was revealed for each of the three data sets (Fig. 3a). The WUE_x was significantly higher for the $Australia_{01–09}$ sites (PDSI = −1.34) than for the $LTER_{75–98}$ and $USDA_{00–09}$ sites (PDSI ≈ 0 and PDSI = −0.81, respectively) ($P < 0.05$, Fig. 3a, inset). This indicates a cross-biome sensitivity to prolonged warm drought

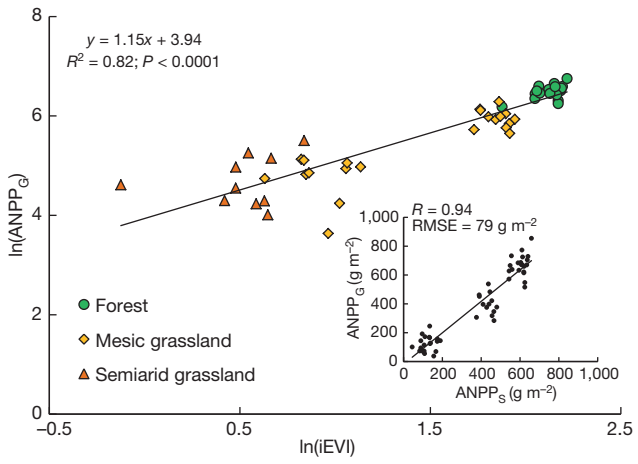

Figure 1 | Relationship between ANPP and iEVI. Relationship between *in situ* estimates of above-ground net primary production ($ANPP_G$) and iEVI derived from MODIS data (2000–2009) for ten sites across several biomes (see Supplementary Information and Supplementary Table 2). The solid line represents the linear regression used to estimate ANPP from iEVI ($ANPP_S$), in which $ANPP_S = 51.42 \times iEVI^{1.15}$. The inset shows the correlation between estimates of $ANPP_S$ and $ANPP_G$ for the ten sites over several years.

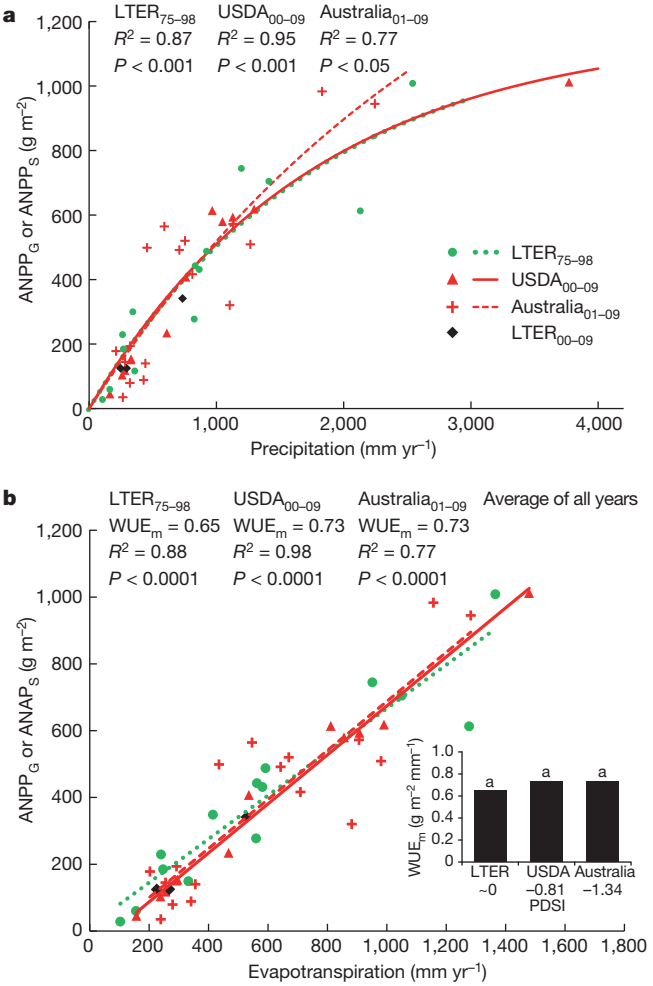

Figure 2 | Cross-biome sensitivity to precipitation during altered hydroclimatic conditions. a, **b**, Relationship of plant production to precipitation (**a**) and evapotranspiration (**b**) across precipitation regimes during the late twentieth century ($LTER_{75–98}$, green) and during altered hydroclimatic conditions characterized by prolonged, warm drought ($USDA_{00–09}$ and $Australia_{01–09}$, red), showing significant coefficients of determination in regressions for each data set. Symbols represent the mean values for each site over multi-year study periods. Three LTER sites with *in situ* estimates of $ANPP_G$ during 2000–2009 (black) were included for qualitative validation of results with $ANPP_S$. The inset in **b** illustrates differences in mean water-use efficiencies (WUE_m: the slope of the ANPP/evapotranspiration relationship) across hydroclimatic conditions, in which PDSI ranged from ~0 to −1.34. Columns labelled with the same letter are not significantly different ($P > 0.05$).

where ecosystems sustain productivity in the driest years by increasing their WUE_e. The increase in cross-biome WUE_x with declining PDSI suggests that most biomes were primarily water limited during the driest years of the early twenty-first century drought, and this overshadowed limitations imposed by other resources even at high-productivity sites.

As a test of ecosystem resilience, a similar comparison was made for the wettest years during the mid- to late-drought (2003–2009) and compared to the results for the wettest years during the earlier hydroclimatic conditions from 1975–1998. For the wettest years in both periods, we found a minimum value (WUE_n) that was common to all biomes and similar across both hydroclimatic periods (Fig. 3b). The finding that WUE_n did not vary ($P > 0.05$) across different hydroclimatic periods indicates a cross-biome capacity to respond to high annual precipitation, even during periods of warm drought. The decrease from maximum to minimum WUE_e ranged from 14% (for the $USDA_{00–09}$ and $LTER_{75–98}$ data sets) to 35% (for the $Australia_{01–09}$ data set) and is thought to occur through additional resource constraints that come into play in wet years, including light and nutrient limitations[10]. However, it may also be true that the mechanistic relationship between the two time periods was not consistent, where shifts in species composition as a result of contemporary drought influenced this landscape-scale process.

The ability of plants to increase WUE_x and retain historic WUE_n during altered hydroclimatic conditions suggests that the factors controlling these two processes are different with respect to how the climate and vegetation assemblage are changing. During the driest years, there was a cross-biome adjustment in WUE_e that increased with drought intensity, thus sustaining production at near late-twentieth-century levels during prolonged drought. In the wettest years, the sites exhibited an ability to absorb the disturbances associated with the early twenty-first century drought and retained the same sensitivity of ANPP to water availability across both hydroclimatic periods. These different responses to precipitation extremes may be due to changes in vegetation structure and function, and to plant–soil feedbacks that are not captured in the integrated analysis of either RUE or WUE_e. These must be considered in a full assessment of ecosystem vulnerability or resistance to change.

In this study, ecosystem resilience was measured as the capacity of ecosystems to absorb disturbances associated with the early twenty-first century drought and retain late-twentieth-century sensitivity of ANPP to high annual water availability. Our analyses suggest an intrinsic sensitivity of plant communities to water availability, and a shared capacity to tolerate low annual precipitation but also to respond to high annual precipitation. These findings provide a conceptual model of ecosystem resilience at the decadal scale during the altered hydroclimatic conditions that are predicted for later this century[1] (Fig. 4). During the driest years, the high-productivity sites became water limited to a greater extent resulting in higher WUE_e similar to that encountered in less productive, more arid ecosystems. It follows that when all ecosystems are primarily water limited, a cross-biome maximum WUE_e will be reached (WUE_x) that cannot be sustained with further reductions in water availability. Furthermore, we predict that as cross-biome WUE_e reaches that maximum WUE_x value, WUE_n will approach WUE_x because production will be limited largely by water supply and less so by nutrients and light (Fig. 4).

With continuing warm drought, the single linear ANPP/evapotranspiration relation that forms the common cross-biome WUE_e would collapse as biomes endure the significant drought-induced mortality

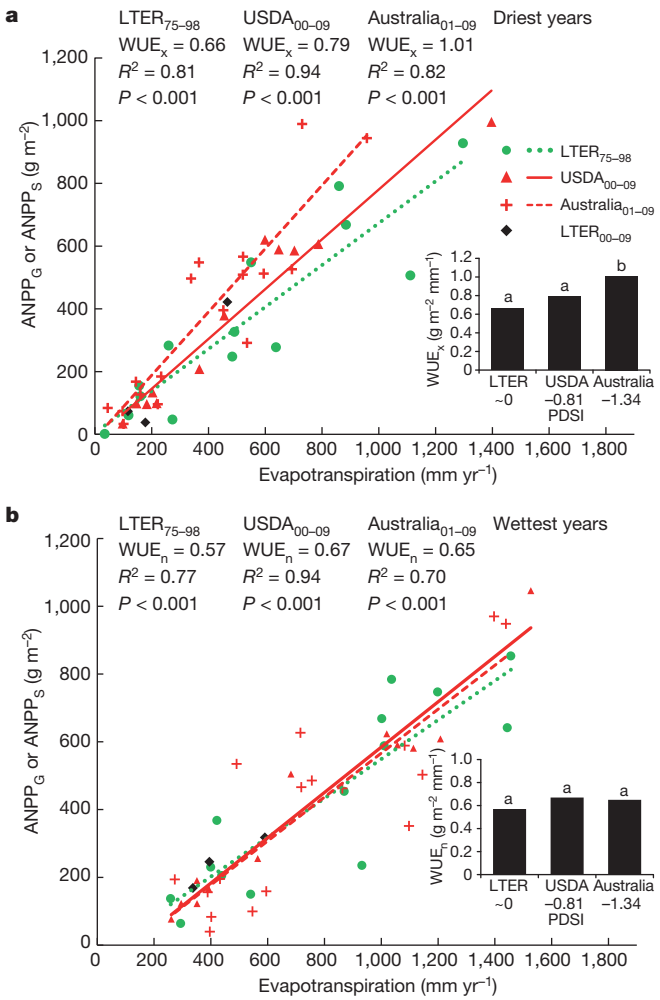

Figure 3 | Ecosystem resilience across biomes and hydroclimatic conditions. **a**, **b**, Maximum (WUE_x) (**a**) and minimum (WUE_n) (**b**) water-use efficiency (slope of the ANPP/evapotranspiration) in the driest and wettest years, respectively, based on all sites for each data set, plus the three $LTER_{00–09}$ validation sites. The insets illustrate the differences in WUE_x (**a**) and WUE_n (**b**) with mean PDSI for the study periods and locations. Columns labelled with the same letter are not significantly different ($P > 0.05$) across hydroclimatic conditions.

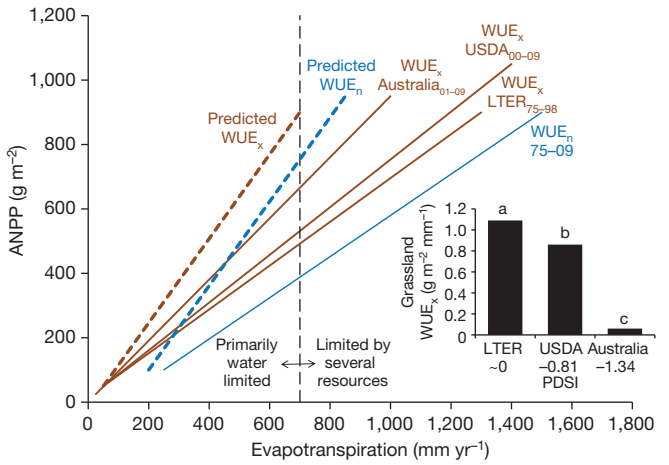

Figure 4 | A conceptual model of ecosystem resilience during altered hydroclimatic condition. A summary of WUE_e results in this study (solid lines), overlain with the predicted behaviour of WUE_x (brown dashed line) and WUE_n (blue dashed line) along a continuum of sites limited primarily by water and by other resources with an arbitrary distinction made here at evapotranspiration = 700 mm yr^{-1} for illustration only (black dashed line). Predictions are based on forecasts of continuing warm drought[1]. The inset illustrates the decrease in WUE_x with PDSI for subsets of the $LTER_{75–98}$ ($n = 4$), $USDA_{00–09}$ ($n = 5$) and $Australia_{01–09}$ ($n = 2$) data sets limited to grassland sites, where columns labelled with the same letter are not significantly different ($P > 0.05$).

that has been extensively documented over the past decade[2,5]. This loss of resilience associated with dieback would probably occur first for ecosystems that respond most rapidly to precipitation variability (that is, grasslands[21]). Thus, the cross-biome ANPP/evapotranspiration relation would become nonlinear as WUE_x and WUE_n approached zero for the most water-limited, low-productivity sites, whereas WUE_e values would be less affected in the high-productivity sites. Subsets of the $LTER_{75–98}$ ($n = 4$), $USDA_{00–09}$ ($n = 5$) and $Australia_{01–09}$ ($n = 2$) data sets limited to grassland sites were used to corroborate this prediction (Fig. 4, inset). During this study period, grassland WUE_x decreased with increasing aridity (decreasing PDSI), indicating a decreasing resilience with prolonged warm drought in these biomes, as predicted. This suggests that these systems are closer to a threshold which, when crossed, will result in biome reorganization.

Here we quantified the effect of the early twenty-first century drought on ecosystem productivity and resilience across many sites on two continents. Cross-biome capacities and sensitivities of production were maintained through prolonged warm drought by increases of WUE_e during the driest years and resilience during wet years indicated by a common WUE_e across both hydroclimatic periods. The conclusions are particularly compelling because they are based on measurements across several biomes with comparisons of multi-year periods of altered hydroclimatic conditions. These findings were extended to predictions that if warm drought continues, considerable mortality (particularly in low-productivity grasslands that are most sensitive to water availability) may threaten ecosystem resilience across biomes given the substantial changes in ecosystem structure. The emergence of these patterns at the spatial and temporal scale at which they were derived requires investigation of the supporting eco-hydrological mechanisms that underlie the complex plant–soil couplings. Spatially, this work represents broad cross-biome behaviour but does not fully represent the complex site-level response to prolonged warm drought. The site-level mechanisms associated with disease, pests, fire, response lags, species replacement and meristem density in forests[2] and grasslands[4,21] complicate specific processes maintaining or affecting cross-biome resilience of ecosystem function. Furthermore, there are predictions of a general biogeochemical resetting as increases in carbon dioxide supply affect many plant and soil processes[22]. Temporally, these predictions of ecosystem resilience were based on behaviour at the scale of a decade or longer, including a period of prolonged warm drought. With careful application of this satellite-based metric, it is possible to continue monitoring cross-biome ecosystem resilience at selected cross-continental sites year-by-year into the future as we develop a greater understanding of the physical and biological mechanisms controlling these patterns.

METHODS SUMMARY

Daily precipitation and temperature were measured at *in situ* stations and represented a homogeneous vegetated area of $\sim 3 \times 3$ km with no major disturbances (for example, fires) during the 2000–2009 period. The total and the mean annual precipitation were computed from daily values over the study period during the hydrological year (October–September for the United States, and May–April for Australia). PDSI values were computed using precipitation, temperature and soil water holding capacity data (see Methods). EVI values were extracted from MODIS images at 250-m spatial resolution for a window size of 9×9 pixels and averaged to one value every 16 days for a time series that was smoothed to obtain iEVI (see Methods). Estimates of annual evapotranspiration were obtained by incorporating annual precipitation and percentages of forested and herbaceous cover in a model derived from more than 250 catchment-scale measurements from around the world[12].

Full Methods and any associated references are available in the online version of the paper.

Received 6 March; accepted 3 December 2012.
Published online 20 January 2013.

1. Dai, A. Drought under global warming: a review. *WIRES Clim. Change* **2,** 45–65 (2011).
2. Breshears, D. D. *et al.* Regional vegetation die-off in response to global-change-type drought. *Proc. Natl Acad. Sci. USA* **102,** 15144–15148 (2005).
3. Saleska, S. R., Didan, K., Huete, A. R. & da Rocha, H. R. Amazon forests green-up during 2005 drought. *Science* **318,** 612 (2007).
4. Scott, R. L., Hamerlynck, E. P., Jenerette, G. D., Moran, M. S. & Barron-Gafford, G. A. Carbon dioxide exchange in a semidesert grassland through drought-induced vegetation change. *J. Geophys. Res.* **115,** G03026 (2010).
5. Allen, C. D. *et al.* A global overview of drought and heat-induced tree mortality reveals emerging climate change risks for forests. *For. Ecol. Manage.* **259,** 660–684 (2010).
6. Milly, P. C. D. *et al.* Stationarity is dead: whither water management? *Science* **319,** 573–574 (2008).
7. Weltzin, J. F. *et al.* Assessing the response of terrestrial ecosystems to potential changes in precipitation. *Bioscience* **53,** 941–952 (2003).
8. Roxburgh, S. H., Berry, S. L., Buckley, T. N., Barnes, B. & Roderick, M. L. What is NPP? Inconsistent accounting of respiratory fluxes in the definition of net primary production. *Funct. Ecol.* **19,** 378–382 (2005).
9. Le Houérou, H. N. Rain use efficiency: a unifying concept in arid-land ecology. *J. Arid Environ.* **7,** 213 (1984).
10. Huxman, T. E. *et al.* Convergence across biomes to a common rain-use efficiency. *Nature* **429,** 651–654 (2004).
11. Monson, R. K. *et al.* Tree species effects on ecosystem water-use efficiency in a high-elevation, subalpine forest. *Oecologia* **162,** 491–504 (2010).
12. Zhang, L., Dawes, W. R. & Walker, G. R. Response of mean annual evapotranspiration to vegetation changes at catchment scale. *Water Resour. Res.* **37,** 701–708 (2001).
13. Walker, B., Holling, C. S., Carpenter, S. R. & Kinzig, A. Resilience, adaptability and transformability in social–ecological systems. *Ecol. Soc.* **9,** 5 (2004).
14. MacDonald, G. M. Water, climate change, and sustainability in the southwest. *Proc. Natl Acad. Sci. USA* **107,** 21256–21262 (2010).
15. National Oceanic and Atmospheric Administration. US climate division data plots (http://www.esrl.noaa.gov/psd/data/usclimdivs) (2012).
16. Jung, M. *et al.* Recent decline in the global land evapotranspiration trend due to limited moisture supply. *Nature* **467,** 951–954 (2010).
17. National Drought Mitigation Center. U.S. drought monitor (http://drought.unl.edu/MonitoringTools/USDroughtMonitor.aspx) (2012).
18. Australian. Government Bureau of Meteorology. Australia's climate change datasets (http://www.bom.gov.au/climate/change/datasets/datasets.shtml) (2011).
19. Huete, A. *et al.* Overview of the radiometric and biophysical performance of the MODIS vegetation indices. *Remote Sens. Environ.* **83,** 195–213 (2002).
20. Running, S. W. *et al.* A continuous satellite-derived measure of global terrestrial primary production. *Bioscience* **54,** 547 (2004).
21. Knapp, A. K. & Smith, M. D. Variation among biomes in temporal dynamics of aboveground primary production. *Science* **291,** 481–484 (2001).
22. Morgan, J. A. *et al.* C4 grasses prosper as carbon dioxide eliminates desiccation in warmed semi-arid grassland. *Nature* **476,** 202–205 (2011).

Supplementary Information is available in the online version of the paper.

Acknowledgements The work was supported in part by the NASA SMAP Science Definition Team under agreement 08-SMAPSDT08-0042, the Australian Research Council (ARC) Discover Project (DP1115479) and the Terrestrial Ecosystem Research Network (TERN) EIF: AusCover. We thank the Australian Bureau of Meteorology for providing the precipitation data. We also thank J. Overpeck, T. McVicar, R. Donohue and M. Walbridge for their input.

Author Contributions G.E.P.C., M.S.M. and A.H. conceived the study, assembled the data and produced the preliminary results. The remaining authors collected and analysed data, and contributed to the interpretation of results. All authors contributed to writing the paper. Statistical analyses were performed by G.E.P.C.

Author Information Reprints and permissions information is available at www.nature.com/reprints. The authors declare no competing financial interests. Readers are welcome to comment on the online version of the paper. Correspondence and requests for materials should be addressed to G.E.P.C. (geponce@gmail.com) or M.S.M. (susan.moran@ars.usda.gov).

METHODS

MODIS iEVI. At each $USDA_{00–09}$ and $Australia_{01–09}$ site (see Supplementary Information and Supplementary Table 1), MODIS EVI (MOD13Q1) data with 16-day and 250-m temporal and spatial resolutions, respectively, were acquired from the corresponding MODIS tiles. Sites were selected where vegetation was uniform across space and *in situ* climate records representative of the location could be obtained. We extracted areas of 2.25 × 2.25 km (9 × 9 250-m pixels) for each location, yielding 23 16-day image files per year for a total of 230 files for each site. Pixel-based quality assurance control was applied to the time series data to remove low-quality, cloud- and aerosol-contaminated pixels and observations made at large sensor zenith angles (>30°). The retained high-quality pixels were averaged to represent the EVI value for that site and 16-day period, resulting in a 10-year EVI time series for each site.

The next step was to use the software tool TIMESAT[23] to smooth the quality-assurance-filtered time series data and standardize the MODIS EVI time series analysis for consistent cross-site comparisons. The TIMESAT filtering option known as the adaptive Savitzky–Golay filter[24] was applied over the time series for smoothing the data and suppressing noise by replacing each data value y_i, $i = 1,...,n$ by a linear combination of nearby values in a window, where

$$\sum_{j=-n}^{n} c_j y_{i+j} \quad (1)$$

and the weights were $c_j = 1/(2n + 1)$, and the data value y_i was replaced by the average of the values in the window. The moving-average method preserved the area and mean position of a seasonal peak, but altered both the width and height. The latter properties were preserved by approximating the underlying data value with the value obtained from a least-square fit to a polynomial, rather than the average in the window. For each data value y_i, $i = 1, 2,\ldots, n$ a quadratic polynomial was fitted as $f(t) = c_1 + c_2t + c_3t^2$ to all $2n + 1$ points in the moving window and the value y_i was replaced with the value of the polynomial at position t_i (ref. 24). The advantage of this method was that it preserved features of the distribution such as relative maxima, minima and width, which were usually 'flattened' by other adjacent-based averaging techniques.

To simplify the process of integrating EVI values from TIMESAT and avoid parameterization, we integrated over the entire year for every site. Therefore, the process of integrating EVI to obtain iEVI was based on using the default parameters found when TIMESAT was initiated. After smoothing the series, we proceeded to extract an offset of 0.05 of each 16-day EVI value to reduce effects of soil exposure. Our process was standardized by applying the same procedures to each data set used.

Meteorological data. Daily precipitation and temperature were measured at *in situ* stations associated with the experimental sites. Total annual precipitation (sum of daily precipitation, mm yr^{-1}), mean annual precipitation (MAP) (mean of annual precipitation over the study period, mm yr^{-1}) and mean maximum temperature (mean of average monthly maximum temperature, °C) were computed for the hydrological year, defined as the 12-month period from October–September in the Northern Hemisphere and May–April in the Southern Hemisphere. The warm season was defined as April–September for USDA sites and November–April for Australia sites.

PDSI. The PDSI[25] was computed with the Thornthwaite equation[26] using a self-calibrating PDSI implementation that automatically calibrated the behaviour of the index at any location[27]. The Thornthwaite equation computes potential evapotranspiration (PET) = $16d(10T/I)^a$, in which T is the mean temperature for the month, d is a correction factor that depends on latitude and month, I is an annual thermal index, and a is an empirical factor[26]. The three main PDSI inputs were monthly rainfall, monthly temperature and soil water holding capacity (SWHC). Rainfall and temperature were obtained from the stations used in this study. We obtained the SWHC data from the NRCS web soil survey (http://websoilsurvey.nrcs.usda.gov/app/WebSoilSurvey.aspx) for the USDA sites and the Australian Soils Resource Information System (ASRIS; http://www.asris.csiro.au/index_other.html) for the Australia sites.

The PDSI is a measure of drought and wet spells, in which PDSI = 0 is normal, −3 is moderate drought, −4 is extreme drought, and excess precipitation is represented by a positive PDSI. We obtained the PDSI for the time period from 1980 to 2009 to identify the average drought conditions across the USDA, LTER and Australia sites. On the basis of this site-specific PDSI (see Supplementary Information and Supplementary Table 3) and reports of continental-scale drought extent and severity[15–18] (summarized in the main text), the period of altered hydroclimatic conditions was determined to be 2000–2009 for USDA sites and 2001–2009 for Australia sites, reflected by the naming convention $USDA_{00–09}$ and $Australia_{01–09}$, respectively.

Evapotranspiration model. Estimates of evapotranspiration at different biomes were obtained using a model of mean annual evapotranspiration formulated with data from more than 250 catchment-scale measurements from around the world[12]. The two-parameter model offers an approach for estimation of mean annual evapotranspiration (ET) on the basis of changes in annual precipitation (P) (mm yr^{-1}) and the percentage of forest cover (f), where

$$\mathrm{ET} = \left(\overbrace{f \frac{1+2\frac{1{,}410}{P}}{1+2\frac{1{,}410}{P}+\frac{P}{1{,}410}}}^{\text{Fractional forest cover}} + \overbrace{(1-f)\frac{1+0.5\frac{1{,}100}{P}}{1+\frac{1{,}100}{P}+\frac{P}{1{,}100}}}^{\text{Fractional herbaceous plants cover}} \right) P \quad (2)$$

The model has two portions as depicted in equation (2), with the left side accounting for the fractional forest cover and the right side accounting for the fractional herbaceous plant cover (non-forested). The main advantage of this model over more traditional models is the derivation from data readily available at the catchment scale. For the $USDA_{00–09}$ data set, the information about the percentage of non-forested areas was obtained from contacts at each location. For the $Australia_{01–09}$ data set, estimations of the percentage of non-forested areas were made using Google Earth.

23. Jönsson, P. & Eklundh, L. TIMESAT–a program for analyzing time-series of satellite s ensor data. *Comput. Geosci.* **30,** 833–845 (2004).
24. Savitzky, A. & Golay, M. J. E. Smoothing and differentiation of data by simplified least s quares procedures. *Anal. Chem.* **36,** 1627–1639 (1964).
25. Palmer, W. C. *Meteorological Drought* Weather Bureau Res. Paper no.45 (1965).
26. Thornthwaite, C. W. An approach toward a rational classification of climate. *Geogr. Rev.* **38,** 55 (1948).
27. Wells, N., Goddard, S. & Hayes, M. J. A self-calibrating Palmer Drought Severity Index. *J. Clim.* **17,** 2335–2351 (2004).